Development of Mathematical Models to Analyse and Predict Weld Bead Geometry and Shape Relationships in FCA Welding of C-45 Mild Steel

Gantavya Vivek Punj[1*], Niyajudin[1] and Pradeep Khanna[2]
[1]Student, [2]Associate Professor
Division of Manufacturing Processes and Automation Engineering,
Netaji Subhas Institute of Technology, Dwarka, New Delhi 110078.
[*]Email: gantavyavpunj@gmail.com

DOI : 10.22486/iwj/2018/v51/i4/176798

ABSTRACT

Welding plays an extremely important role in fabrication industry because of its adaptability to automation, relative simplicity, strong and reliable joints and ability to weld a large variety of materials making it widely acceptable in construction, transport, automotive and pressure vessel industry. A wide variety of arc welding processes are available to cater to the needs of ever increasing industrial demands. GMAW is one such arc welding process which has proved its significance in industry owing to its versatility and quality of joints. The physical dimensions and shape of a weld joint not only decides its mechanical strength but also affects its performance during service. Sufficient knowledge of various bead parameters such as penetration, reinforcement, width, etc. becomes imperative along with their dependence on various welding parameters constituting voltage, feed rate of wire and speed of welding. In the present research work, an attempt was made to form a mathematical model for bead geometry prediction at given values of weld input parameters. Statistical techniques have been applied for the present investigation work.

Keywords: ANOVA; Design of experiments; Wire feed rate; Weld Dilution; GMAW welding.

1.0 INTRODUCTION

Metal Inert Gas welding is one of the most fundamental and most applied processes in a manufacturing environment amongst the various manufacturing processes [1]. The process has proved its worth in fabrication industry owing to its versatility and the quality of joints. The process lends itself to full automation thereby becoming suitable for mass manufacturing units as well. The physical strength and service performance of the welds depend upon the weld bead shape and geometry, which further is decided by response parameters like depth of penetration (p), weld width (w) and height of reinforcement (h). The other related parameters of importance are weld penetration shape factor (WPSF), weld reinforcement form factor (WRFF) and weld dilution (D). To have a weld joint of desired strength, a specific combination of these parameters is required [2]. The input parameters like arc voltage, speed of welding, current, etc. are found to have an effect on bead geometry parameters mentioned above [3]. As already mentioned, these response parameters constitute the bead shape which is of prime significance while deciding the mechanical strength of the welded joint. Secondly, when the welding is carried out by robots, it becomes necessary to feed various input parameters into the system to have desired bead shape to have optimum performance in service. This necessitates a detailed investigative work to be carried out with a view to create a mathematical model to relate input and output parameters so that within the working range, for any combination of input welding parameters, optimum responses are obtained.

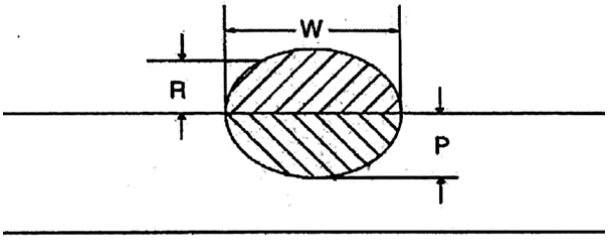

Fig. 1A : Cross section of a theoretical weld bead

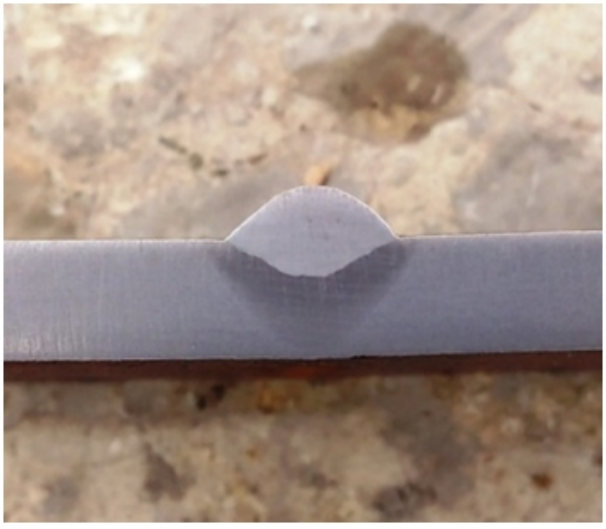

Fig. 1B : Image of an actual weld bead

Fig. 1A shows the schematic whereas **Fig. 1B** shows the actual weld bead photograph.

The mathematical model was developed by using the design of experiments where the method of central composite rotatable design was utilized to conduct the experiments [4]. Investigation of Variance method was used to check the significance of the models and t-test was used to test the significance of model coefficients [5]. The model was optimized by response surface methodology.

2.0 EXPERIMENTAL SETUP

The present investigation work was carried out on a MIG welding power source of capacity 400 A, 60% duty cycle with flat V-I characteristics. A flux cored wire of 1.2 mm diameter was used with carbon dioxide as shielding gas. A mechanised carriage unit was used to ensure consistent and reproducible welds at the same time eliminating the weld quality variation that inadvertently creeps in during manual welding. The complete setup used for the purpose is shown in **Fig. 2**.

Fig. 2 : The complete welding setup

3.0 PLAN OF INVESTIGATION

The research work was proceeded according to the steps mentioned below:

1. Recognition of input factors and finding their working limits
2. Developing design matrix
3. Performing experiments according to the designed matrix
4. Developing of mathematical models
5. Testing adequacy of the designed models
6. Checking the importance of regression coefficients
7. Investigation of results

3.1 Recognition of Input Factors and Finding Their Working Limits

A number of trial experimental runs were made to identify the input parameters that affect the response parameters most significantly [6]. It was found that out of many input parameter options available, the ones that significantly affected the bead shape are wire feed rate (WFR), arc voltage (V), welding speed (S), nozzle to plate distance (NPD) and torch angle (Φ). The weld pieces were subjected to visual checking for the following to decide upon the operating limits of the input parameters,

1. The bead is visually of good quality
2. No spatters
3. No cracks or undercuts

3.2 Developing the Design Matrix

A design matrix was developed by following the central composite rotatable design technique for five variables with 32 experimental runs. The breakup of these runs is 2^{5-1}=16

fractional factorial runs plus 2*5=10 star points plus 6 centre points. On conducting all the trial tests, the working limits of parameters which came are given in **Table 1**. Upper limits were coded as +two and lower limits as -two.

Table 1: Input parameters and their operating ranges

Parameter	Unit	Los (-2)	High (+2)
WFR	m/min	3	9
Voltage	V	14	22
NPD	mm	10	20
Torch Angle	degrees	70	110
Welding Speed	cm/min	25	45

3.3 Performing Experiments According to the Designed Matrix

According to the design matrix, 32 experimental runs were carried in an arbitrary manner to eliminate any kind of precise mistake in the machine. For different combinations of input parameters, according to the design matrix the corresponding response parameters were recorded in **Table 2**.

3.4 Developing the Mathematical Models

The response function which gives information about the bead shape can be communicated as:

Y = f (A, B, C, D, E), where Y = Response variable, A = Wire feed rate (m/min), B= Voltage (V), C= Nozzle to plate distance (mm), D= Torch angle (degree), E= Welding speed (cm/min)

General Equation for the present case can be presented as:

$B_0+\beta_{12}AB+\beta_{13}AC+\beta_{14}AD+\beta_{15}AE+\beta_{23}BC+\beta_{24}BD+\beta_{25}BE+\beta_{34}CD+\beta_{35}CE+\beta_{45}DE+\beta_{11}A^2+\beta_{22}B^2+\beta_{33}C^2+\beta_{44}D^2+\beta_{55}E^2$

3.5 Testing Adequacy of the Designed Model

Investigation of Variance technique was utilized to check the adequacy of the model [7]:

(I) the standard tabulated value for required amount of confidence should be more than that of the calculated value of F-ratio [8].

(II) For a confidence amount required, the standard tabulated value should be more than the calculated R-ratio value. It might be expected that the model was sufficient within as far as possible [8].

The tabulated value of F-ratio and R-ratio was 4.95 and 4.56 respectively,

$$\text{F-ratio} = \frac{\text{(Mean Square of lack of fit)}}{\text{(Mean Square of error)}}$$

$$\text{R-ratio} = \frac{\text{(Mean Square of (1st order terms+2nd order terms)}}{\text{(Mean Square of error)}}$$

From the **Table 3**, it becomes clear that all the models are acceptable.

3.6 Checking the Importance of Regression Coefficients

Testing the significance of the regression coefficients is required as to decide the number of terms to be retained in the model to keep it of reasonable length and still accurate. This can be done by dropping the non significant terms without sacrificing the adequacy of the model formed. T-test was used for this purpose where the tabulated and calculated values of t were compared and the coefficients whose calculated values exceeded the standard tabulated values were retained and the remaining were dropped [9]. Given below are the mathematical models developed after conducting this analysis.

Depth of penetration = 2.42A+0.23A+0.13B-0.22C-0.08D-0.06E+0.10AB-0.07AC-0.03AD+0.03AE-0.13BC-0.02BD-0.02BE+0.01CD-0.03CE-0.14DE-0.09A^2-0.25B^2+0.03C^2-0.09D^2-0.07E^2

Weld width = 11.16+0.41A+1.25B+0.20C-0.49D-0.78E+0.19AB+0.11AC-0.34D+0.29AE-0.13BC+0.15BD+0.26BE-0.31CD+0.24CE-0.24DE-0.42A^2-0.42B^2-0.26C^2-0.07D^2-0.22E^2

Height of reinforcement = 3.00+0.50A-0.35B0.01C+0.10D-0.09E-0.12AB0.04AC+0.08AD+0.01AE+0.04BC-0.06BD+0.08BE+0.08CE+0.04DE-0.01A^2-0.01B^2+0.04C^2-0.09D^2-0.01E^2

Weld dilution = 41.55-0.98A+5.89B-2.77C-0.52D+ 0.71E+2.20AB+0.06AC+0.65AD-0.29AE-1.53BC+2.06BD-2.30BE-1.47CD+2.61CE-2.21DE-0.18A^2-2B^2+1.12C^2-0.44D^2-0.30E^2

Weld penetration shape factor (WPSF) = 4.64-0.35A+0.35B+0.58C-0.06D-0.2E-0.15AB+0.17AC-0.06AD+0.1AE+0.28BC+0.15BD+0.31BE-0.19CD+0.22CE+0.19DE+0.07A^2+0.42B^2-0.09C^2+0.15D^2+0.02E^2

Weld reinforcement form factor (WRFF)= 3.76-0.42A+0.84B+0.06C-0.28D-0.16E+0.02AB+0.07AC-0.12AD+0.06AE-0.06BC+0.02BD+0.03BE-0.23CD+0.14CE-0.12DE-0.05A^2-0.01B^2-0.15C^2+0.08D^2-0.09E^2

Table 2 : Design matrix and measured values of bead shape parameters

RUNS	WFR	V	NPD	Φ	S	p	w	h	D	WPSF	WRFF
	m/min	V	mm	degrees	cm/min	mm	mm	mm	%		
1	9	18	15	90	35	2.7	9.9	4	39.6	3.57	2.4
2	6	18	15	70	35	2.4	12	2.5	40.2	5	4.65
3	7.5	20	17.5	100	40	1.5	10.3	3.1	41.6	6.86	3.32
4	3	18	15	90	35	1.6	9.2	2	42.2	5.75	4.6
5	4.5	20	17.5	100	30	1.6	10.4	2.4	40.2	6.5	4.33
6	6	14	15	90	35	1.1	6.3	3.8	21.1	5.72	1.65
7	7.5	16	17.5	100	30	1.8	8.8	4.3	22.9	4.88	2.04
8	4.5	16	12.5	100	30	1.8	10.1	2.7	37.9	5.6	3.74
9	7.5	16	12.5	100	40	1.8	6.7	4.1	29	3.72	1.63
10	6	18	20	90	35	2.2	11.1	3.3	39.7	5	3.36
11	7.5	20	12.5	80	40	2.9	11.5	2.9	44.8	3.88	3.96
12	4.5	16	12.5	80	40	1.8	6.8	2.4	43.4	3.77	2.83
13	6	18	15	90	45	2.1	8.9	2.9	41.4	4.23	3.06
14	7.5	20	17.5	80	30	1.9	12.3	2.8	38.8	6.47	4.39
15	6	18	15	90	25	2.5	11.8	3.2	39.4	4.72	3.68
16	6	18	10	90	35	3.2	9.3	3.2	52.5	2.88	2.9
17	4.5	16	17.5	80	30	1.6	9.9	2.7	32.9	6.18	3.66
18	4.5	20	12.5	100	40	1.6	9.2	2.1	44.7	5.75	4.38
19	4.5	20	12.5	80	30	1.9	10.7	2.2	47.9	5.63	4.86
20	6	18	15	90	35	2.9	11.4	3.2	43.6	3.93	3.56
21	4.5	16	17.5	100	40	1.4	6.4	2.5	35.2	4.57	2.56
22	6	18	15	90	35	2.4	12.5	2.8	42.4	5.2	4.46
23	4.5	20	17.5	80	40	1.4	9.7	2	44.6	6.99	4.98
24	7.5	20	12.5	100	30	2.6	11.8	2.9	60.5	4.41	4.06
25	7.5	16	12.5	80	30	1.9	10.1	3.9	29.8	5.31	2.58
26	6	18	15	90	35	2.2	10.5	3.15	39.7	4.6	3.35
27	6	18	15	110	35	2	9.9	2.8	39.4	4.95	3.53
28	6	18	15	90	35	2.3	11.2	2.9	41.2	4.86	3.86
29	7.5	16	17.5	80	40	1.9	10.3	3	40.9	5.42	3.39
30	6	18	15	90	35	2.1	11.2	2.7	42.4	5.33	4.14
31	6	22	15	90	35	2	12.8	2.2	46.1	6.4	5.81
32	6	18	15	90	35	2.2	9.9	3.1	39.8	4.5	3.19

Table 3: Checking the adequacy of developed models

Bead geometry parameters	First-order terms		Second-order terms		Lack of fit		Pure error		F-ratio	R-ratio	R^2-value	Adequacy of the models
	S.S	df	S.S	df	S.S	df	S.S	df				
Depth of penetration	3.27	5	3.67	15	0.54	6	0.39	5	1.15	6.03	0.88	Adequate
Weld width	63.12	5	22.85	15	3.32	6	3.79	5	0.73	65.62	0.92	Adequate
Height of reinforcement	9.52	5	1.23	15	0.15	6	0.21	5	0.59	160.4	0.97	Adequate
Weld dilution	1058.68	5	660.17	15	7.32	6	12.18	5	0.5	469.63	0.99	Adequate
Weld penetration shape factor	15.32	5	15.39	15	2.18	6	1.31	5	1.39	49.53	0.89	Adequate
Weld reinforcement form factor	23.99	5	3.2	15	0.64	6	1.18	5	0.45	79.5	0.94	Adequate

3.7 Investigation of Results

The mathematical models which have been developed above can act as a powerful tool to estimate bead geometry and shape connections for the welding parameters utilized as a part of examination by putting their specific quantities in coded frame [10]. According to these models, direct as well as interaction impacts of all procedure parameters on bead geometry were evaluated and plot is shown in **Fig. 3** through **Fig. 19**.

3.7.1 Direct Impacts of Welding Variables

Direct impact of welding parameters on the reactions refer to impact of a single parameter has on the response during its operating range while keeping the other parameters constant.

3.7.1.1 Direct Impact of (WFR) on Weld Bead Parameters

It is apparent from **Fig. 3** that on increasing WFR, a constant linear increase is observed in penetration. The reason could be attributed that as welding current and wire feed rate have a direct linear relation, an increment in welding current leads to increase in the line energy per unit length of the weld bead as well as enhanced current density leading to higher amount of melting of the base metal resulting in increased penetration. Moreover, Welding current has a direct impact on energy of the droplets as well when it hits to the weld pool leads to increase in penetration. For reinforcement, it is obvious that on increasing WFR, reinforcement is also increasing. It can be because as WFR increases, there is an increase in temperature of the arc due to rise in current due to which wire metal receives high amount of heat thus resulting in metal piling on work piece thus increasing the reinforcement. On coming to

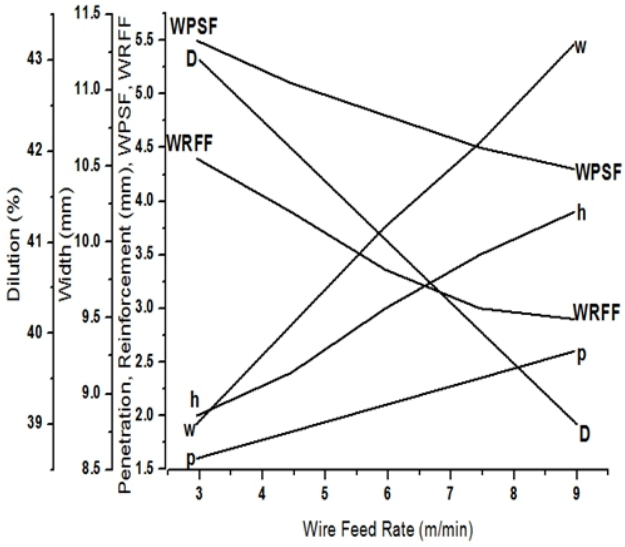

Fig. 3: Direct impact of (WFR) on weld bead parameters

width, a strong constant linear increase is observed, which can be because at greater WFR values, the increase in heat causes two impacts, one it spreads the arc force on a wider area. Secondly it melts more base metal and filler wire which are distributed on a wider area increasing the width. Further it was noted that in dilution, a decrease is seen. It can be because with increment in heat input, it seems that the increase in bead area pre-dominated the increase in penetration area. WPSF and WRFF decreased with rise in WFR. It was due to the reason that at greater amount of current, the rate at which penetration and reinforcement increased was higher than the rate at which width increased.

3.7.1.2 Direct Impact of Voltage (V) on Weld Bead Parameters

It is quite apparent from **Fig. 4** that on increasing voltage, an increase is observed in penetration. It can be because of the fact that as voltage increases, the arc length increases and more melting of base metal took place due to the spread out of arc cone at base leading to increased penetration. Similar increasing impact of voltage on weld width is observed which can due to the reason that the increase in heat which takes place causes two impacts, one it spreads the arc force on a wider area. Secondly it melts more base metal and filler wire which are distributed on a wider area increasing the width. A decreasing trend was observed in reinforcement because with rise of voltage, the arc possesses a tendency to spread at its base resulting in decreased reinforcement. Dilution was observed to increase with rise in voltage. It can be because of the fact that with rise in heat input it seems that increase in penetration pre-dominated the increment in bead area. Increment in WRFF was also seen because width increased but reinforcement decreased. WPSF decreased because with the increase in voltage, the width increased but the rate at which penetration increased seem to dominate.

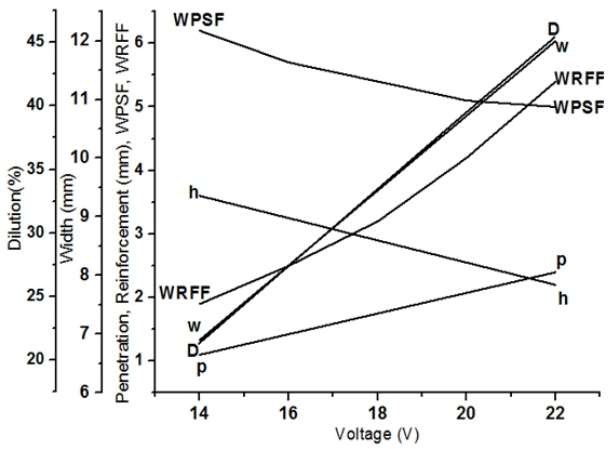

Fig. 4 : Direct impact of Voltage on weld bead parameters

3.7.1.3 Direct Impacts of (NPD) on Bead Parameters

It is apparent from **Fig. 5** that on increasing NPD, a decrease is observed in penetration. It can be stated that on increasing NPD, the distance between work piece and nozzle increases leading to preheating of the wire metal. So, the heat required to melt the work piece gets utilised in melting the wire spool which results in metal piling on the work piece and thus the penetration is decreased. Width also increased with increase in

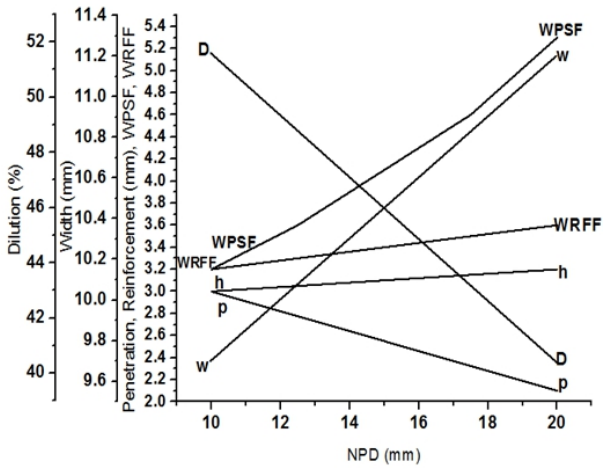

Fig. 5 : Direct impact of (NPD) on weld bead parameters

NPD. It can be due to the reason that the increase in NPD spreads the arc force on a wider area. Reinforcement increased with NPD, which can be because at higher heat input, the wire metal on receiving more heat increases the metal piling resulting in increased reinforcement. The decreasing trend was also observed in dilution. It can be because as NPD increases, the rate of increment in bead area pre-dominated the rate of increment in penetration area. WPSF and WRFF increased with increase in NPD because, when penetration decreased, width was increasing whereas reinforcement increased was lower than the rate at which width increased. The above analysis can now be concluded.

3.7.1.4 Direct Impacts of Torch Angle (Φ) on Weld Bead Parameters

It is apparent from **Fig. 6** that initially, slight increasing impact is observed in penetration and finally a decreasing trend is seen. It can be because at greater angles, the arc force spreads the arc ahead of the weld pool causing an overall spread rather than penetration. An increase in width is also observed which can be due to the reason that at higher torch angles, the thermal energy offered by the arc is not concentrated, which leads to spreading of the bead resulting in increased width. It is apparent from the figure that initially an increase is observed in reinforcement and then a slight decrease is seen. It can be due to the fact that as angle increases, the arc force spreads it resulting in lower reinforcement. Moreover initially an increase is seen in dilution but at higher angles, decrease was observed. It can be because at greater torch angle, the rate of increment in bead area pre-dominated the increment in area of penetration. Initially a decrease is observed in WPSF but for

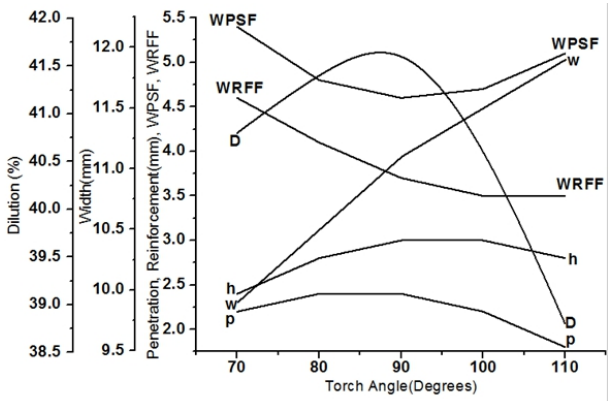

Fig. 6 : Direct impact of torch angle (Φ) on weld bead parameters

angles beyond 90degrees, increase in WPSF is seen due to the fact that initially penetration first increases and then decreases. Moreover decrease in WRFF was also observed as width was always decreasing, but reinforcement was initially increasing and finally decreasing.

3.7.1.5 Direct Impacts of Welding Speed(S) on Weld Bead Parameters

The **Fig. 7** shows that on increasing welding speed, a decrease was observed in case of penetration. It can be because at greater values of welding speed, time required for melting of the base metal becomes less resulting in lesser penetration of the work piece. Width also decreased which can be because of the reason that increment in speed caused less heat per unit length of the weld. Similar reason can be stated for trend observed in reinforcement that insufficient time for the filler metal to melt resulting in lesser reinforcement. An increase was observed in dilution on increasing welding speed. It can be because for higher speeds, rate of increment in penetration

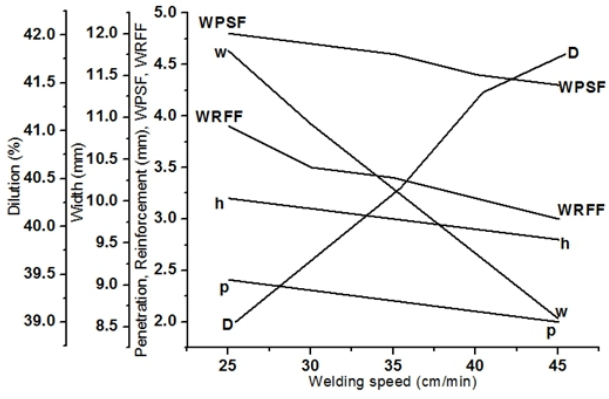

Fig. 7 : Direct impact of welding speed on weld bead parameters

area dominated the increase in total bead area. WPSF and WRFF decreased due to rise in welding speed because rate of decrease in width was higher than rate of decrease in penetration and reinforcement.

3.7.2 Interaction Impacts of Welding Variables

Interaction impact of welding parameters on the reactions refers to the effect of two parameters on a particular response during their operating range while keeping the other parameters constant.

3.7.2.1 Interaction Impact of (WFR) and Welding Speed (S) on Depth of Penetration (p)

Fig. 8 shows that WFR had an increasing impact on depth of penetration whereas welding speed had the opposite impact. The reason could be attribute that with increase in WFR, the heat input per unit length of the weld increased; also there was an increase in the arc force which leads to greater depths of penetration. By the increment in Welding speed on the other hand less time was available for the heat to penetrate the base metal, thereby reducing the depth. The above analysis can now be concluded.

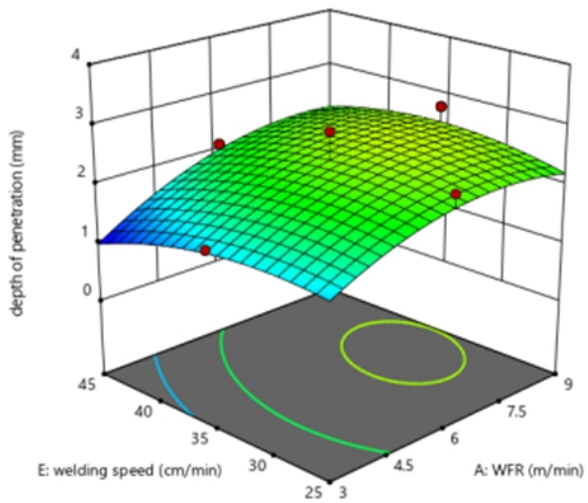

Fig. 8: Interaction impact of WFR and welding speed on depth of penetration

3.7.2.2 Interaction Impact of (WFR) and Torch Angle (Φ) on Depth of Penetration (p)

Fig. 9 shows that on increasing torch angle initially WFR had an increasing impact on penetration whereas torch angle had a decreasing impact on penetration. For torch angles up to 90 degrees, on increasing WFR, there is an increase in penetration because of increased plasma force due to

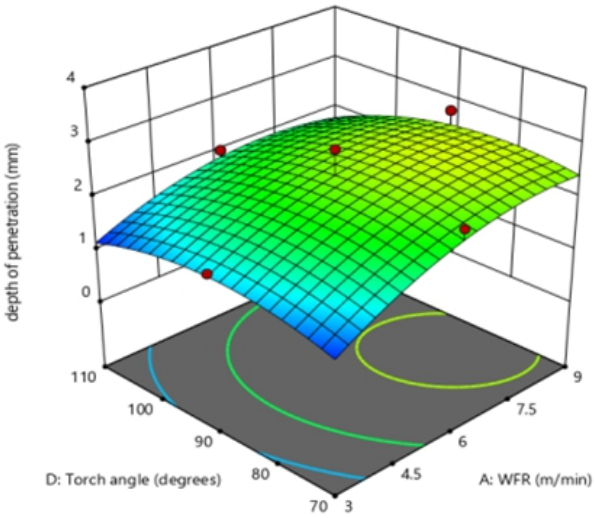

Fig. 9 : Interaction impact of WFR and torch angle on depth of penetration

increased current. For torch angles higher than 90 degrees, on increasing WFR, penetration first increases and then decreases. The reason could be attribute that at higher torch angles, the plasma force leads to spreading of the weld bead at the expense of penetration.

3.7.2.3 Interaction Impact of (WFR) and Welding Speed (S) on Weld Width (w)

It is apparent from **Fig. 10** that for all values of speed, the width first increased and then decreased with the increase in WFR. The reason could be assigned out to the way that with initial increment in WFR, the energy input increase which increased the width, but with further increase in WFR, the arc force became so intense that it had more of a penetrating effect rather than a widening effect.

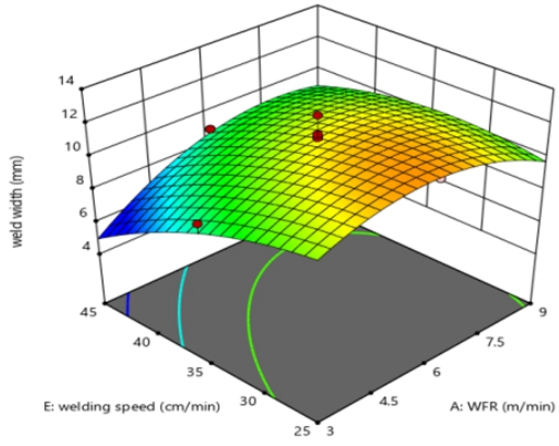

Fig. 10 : Interaction impact of WFR and welding speed on weld width

3.7.2.4 Interaction Impact of Voltage (V) and (NPD) on Weld Width (w)

Fig. 11 shows that voltage had an increasing impact on weld width and also NPD shows the same trend. It can be due to the fact that voltage as well as NPD has an arc widening impact that leads to increment in weld width.

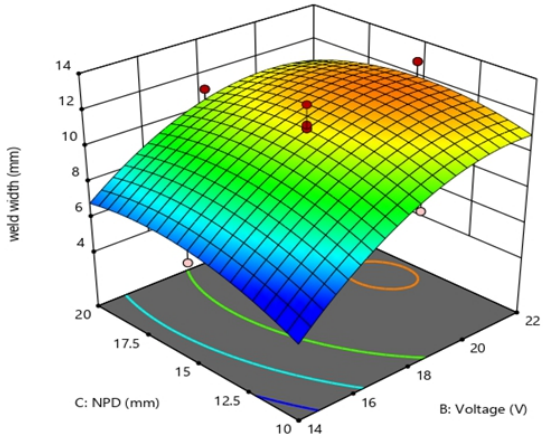

Fig. 11 : Interaction impact of Voltage and NPD on weld width

3.7.2.5 Interaction Impact of (WFR) and Voltage (V) on Height of Reinforcement (h)

Fig. 12 shows that WFR had a positive effect on height of reinforcement whereas voltage had a negative effect. The reason could be assigned that the increase in voltage resulted in the widening of bead thereby reducing the height of reinforcement whereas the increase in WFR has increased the heat input resulting in more filler wire melting making the reinforcement to increase.

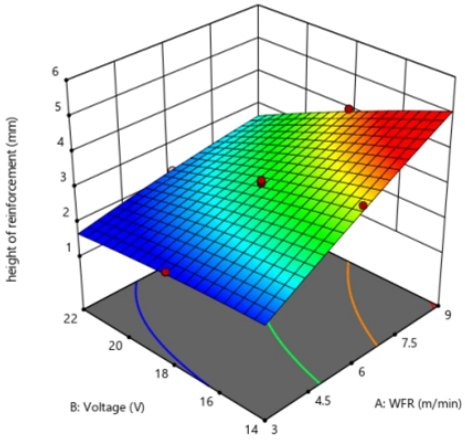

Fig. 12 : Interaction impact of WFR and Voltage on height of reinforcement

3.7.2.6 Interaction Impact of Voltage (V) and (NPD) on Height of Reinforcement (h)

Fig. 13 shows that NPD had a positive effect on height of reinforcement whereas voltage had a negative impact. The reason could be assigned that voltage had a widening impact on the welding arc whereas increase in NPD causes more filler metal piling effect that leads to increase in height of reinforcement.

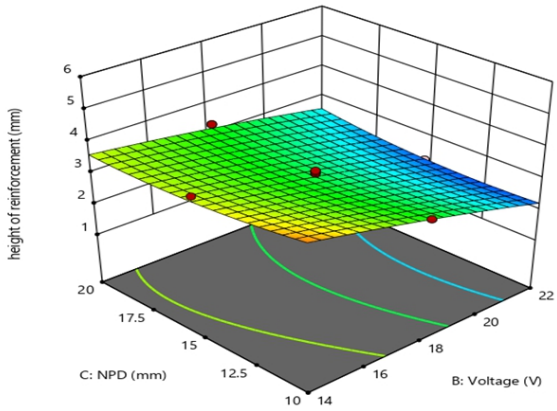

Fig. 13 : Interaction impact of Voltage and NPD on height of reinforcement

3.7.2.7 Interaction Impact of (WFR) and Voltage (V) on Weld Dilution (D)

Fig. 14 shows that voltage had an increasing impact on the dilution whereas WFR had an opposite impact. The reason could be attributed that with increased voltage the total increase in weld bead area was less prominent than the increase in penetration area. With the increase in WFR on the other hand, the increase in bead area could have been more prominent than the penetration area. The above analysis can now be concluded.

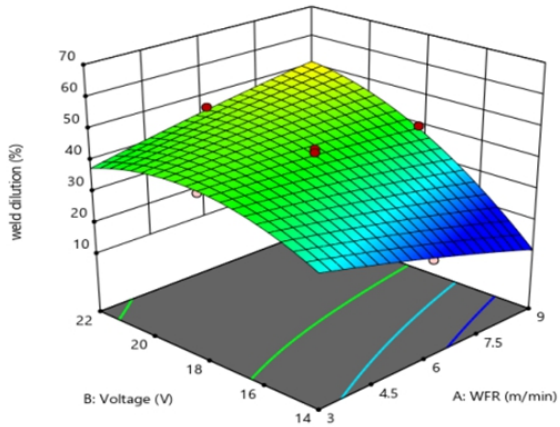

Fig. 14 : Interaction impact of WFR and Voltage on weld dilution

3.7.2.8 Interaction Impact of Voltage (V) and Torch Angle (Φ) on Weld Dilution (D)

Fig. 15 shows that voltage had an increasing impact on dilution whereas torch angle had an opposite impact. It can be due to the reason that with increased voltage the total increase in total weld bead area was less prominent than increase in penetration area. On the other hand, with the increase in torch angle, increase in bead area is more prominent than penetration area.

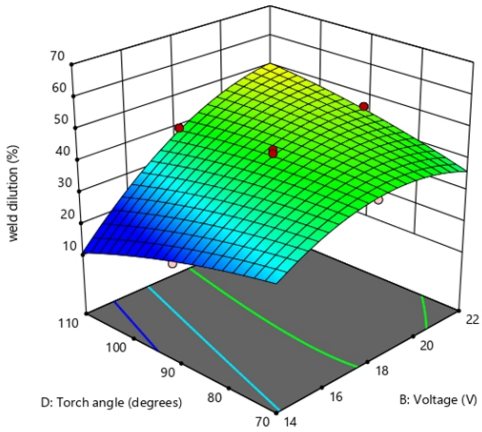

Fig. 15 : Interaction impact of Voltage and Torch angle on weld dilution

3.7.2.9 Interaction Impact of (WFR) and (NPD) on Weld Penetration Shape Factor (WPSF)

Fig. 16 shows that NPD had an increasing impact on WPSF whereas WFR had an opposite impact on WPSF. It can due to the reason that for greater values of WFR, the increment in penetration pre-dominates the increment in width. The increase in width pre-dominates the increment in penetration at the greater values of NPD.

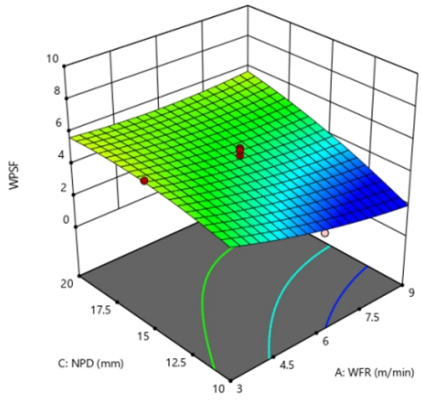

Fig. 16 : Interaction impact of WFR and NPD on WPSF

3.7.2.10 Interaction Impact of (NPD) and Torch Angle (Φ) on Weld Penetration Shape Factor (WPSF)

Fig. 17 shows that NPD had a positive effect on the WPSF and torch angle also shows the same trend. It can be due to the fact that at greater values of both NPD and torch angle, the increase in width pre-dominates the increase in penetration.

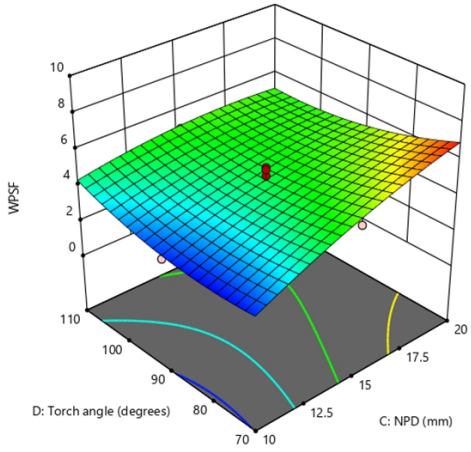

Fig. 17 : Interaction impact of NPD and Torch angle on WPSF

3.7.2.11 Interaction Impact of(WFR) and Voltage (V) on Weld Reinforcement Form Factor (WRFF)

Fig. 18 shows that voltage had an increasing impact on WRFF whereas WFR had an opposite impact [10]. The reason could be attributed that for greater values of WFR, the increase in height of reinforcement is more prominent than the increment in width. The increment in width is more prominent than increment in height of reinforcement at greater values of voltage. The above analysis can now be concluded.

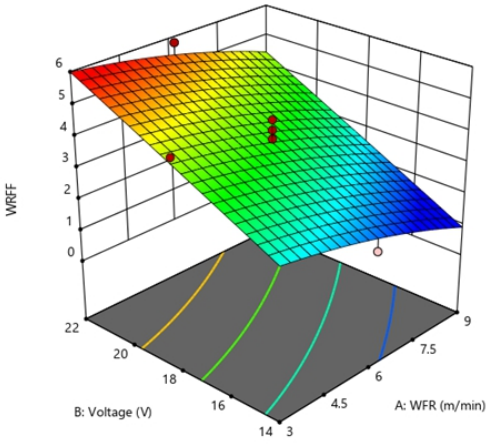

Fig. 18 : Interaction impact of WFR and Voltage on WRFF

3.7.2.12 Interaction Impact of Voltage (V) and (NPD) on Weld Reinforcement Form Factor (WRFF)

Fig. 19 shows that voltage had a positive effect on WRFF and shows the same trend with NPD. It reason could be attributed that for greater values of both voltage and NPD, the rise in width pre-dominates the increase in reinforcement.

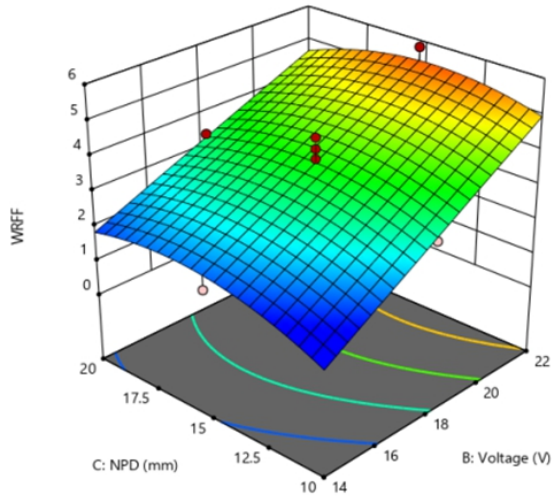

Fig. 19 : Interaction impact of Voltage and NPD on WRFF

4.0 CONCLUSIONS

The research work proceeds out and deduced the conclusions which are mentioned below:

- Central composite rotatable design technique was found useful for the formation of the mathematical models for estimating weld bead measurements and various shape associations under the specified range of process variables.
- Wire feed rate was found to have a positive impact on penetration and height of reinforcement. Penetration was increased to about 2mm when WFR was increased to its maximum(+2) limit. However, negative impact of WFR was observed on weld width.
- Voltage showed a increasing impact on depth of penetration and weld width. However, its decreasing impact was observed in case of height of reinforcement.
- (NPD) showed a decreasing impact on depth of penetration. However its slight increasing impact was observed in cases of reinforcement and weld width.
- Torch angle showed a significant increasing impact in case

of weld width. However, it had a decreasing impact on depth of penetration and height of reinforcement for higher angles.

- Welding speed had a decreasing impact on penetration and shows the same trend with width as well as reinforcement.

REFERENCES

[1] Ghogale MM and Patil SA (2013); Optimisation of process parameters of MIG welding to improve quality of weld by using Taguchi methodology, International Journal of Engineering Research and Technology, 2(12), pp.3677-3685.

[2] Welding Handbook (1978); American Welding Society, 2(2).

[3] Ghosh A and Hloch S (2013); Prediction and optimization of yield parameters for submerged arc welding process, Technical Gazette, 2(20), pp.213-216.

[4] Mishra D, Manjunath A and Parthiban K (2017); Interpulse TIG welding of titanium alloy (Ti-6Al-4V), Indian Welding Journal, 50(4), pp.56-71.

[5] Irfan S and Achwal V (2014); An experimental study on the effect of MIG welding parameters on the weldability of galvanized steel, International Journal on Emerging Technologies, 5(1), pp.146-152.

[6] Gupta VK and Parmar RS (1986); Fractional factorial technique to predict dimensions of the weld bead in automatic submerged arc welding, Journal of Institution of Engineers (India), Mechanical Engineering Division, 70, pp.67-71.

[7] Davies OL (1978); The Design and Analysis of Industrial Experiments, Second edition Longman Press, New York.

[8] Murugan N and Gunaraj V (2005); Prediction and control of weld bead geometry and shape relationships in submerged arc welding of pipes, Journal of Materials Processing Technology, 168(3), pp. 478-487.

[9] Kamble AG and Rao RV (2013); Experimental investigation on the impacts of process parameters of GMAW and transient thermal analysis of AISI321 steel, Advances in Manufacturing, 1(4), pp.362-377.

[10] Kannan T (2009); Effect of process parameters on clad bead geometry and its shape relationships of stainless steel claddings deposited by GMAW, International Journal of Advanced Manufacturing Technology, 47(9-12), pp.1083-1095.